Mammalian cells preferentially internalize hydrogel nanodiscs over nanorods and use shape-specific uptake mechanisms

Rachit Agarwal[a], Vikramjit Singh[b], Patrick Jurney[b], Li Shi[b], S. V. Sreenivasan[b], and Krishnendu Roy[a,1,2]

Departments of [a]Biomedical Engineering and [b]Mechanical Engineering, The University of Texas at Austin, Austin, TX 78712

Edited by W. Mark Saltzman, Yale University, New Haven, CT, and accepted by the Editorial Board September 13, 2013 (received for review March 19, 2013)

Size, surface charge, and material compositions are known to influence cell uptake of nanoparticles. However, the effect of particle geometry, i.e., the interplay between nanoscale shape and size, is less understood. Here we show that when shape is decoupled from volume, charge, and material composition, under typical in vitro conditions, mammalian epithelial and immune cells preferentially internalize disc-shaped, negatively charged hydrophilic nanoparticles of high aspect ratios compared with nanorods and lower aspect-ratio nanodiscs. Endothelial cells also prefer nanodiscs, however those of intermediate aspect ratio. Interestingly, unlike nanospheres, larger-sized hydrogel nanodiscs and nanorods are internalized more efficiently than their smallest counterparts. Kinetics, efficiency, and mechanisms of uptake are all shape-dependent and cell type-specific. Although macropinocytosis is used by both epithelial and endothelial cells, epithelial cells uniquely internalize these nanoparticles using the caveolae-mediated pathway. Human umbilical vein endothelial cells, on the other hand, use clathrin-mediated uptake for all shapes and show significantly higher uptake efficiency compared with epithelial cells. Using results from both upright and inverted cultures, we propose that nanoparticle internalization is a complex manifestation of three shape- and size-dependent parameters: particle surface-to-cell membrane contact area, i.e., particle–cell adhesion, strain energy for membrane deformation, and sedimentation or local particle concentration at the cell membrane. These studies provide a fundamental understanding on how nanoparticle uptake in different mammalian cells is influenced by the nanoscale geometry and is critical for designing improved nanocarriers and predicting nanomaterial toxicity.

cell-uptake mechanism | nanoimprint lithography | drug delivery

Polymeric nanoparticles are widely studied for delivering therapeutic and imaging payloads to cells. Understanding how particle properties affect cell uptake is not only critical for designing improved therapeutic and diagnostic agents (1, 2) but also essential for efficient in vitro cell manipulation (3) and evaluating nanomaterial toxicity (4). Nanoparticle uptake by cells has been shown to depend on particle size, surface charge, and material compositions (5–7). Recent advances in fabrication technologies have enabled generation of shape-specific microparticles and nanoparticles (8–12). These particles, inspired by the diverse, evolutionarily conserved shapes of pathogens and cells, are being used to study the role of carrier shape on cellular internalization, in vivo transport, and organ distribution (6, 11, 13–23).

Despite these pioneering studies, there remains a significant knowledge gap in our fundamental understanding of the interplay between nanoscale shape and size on cellular internalization, especially for clinically relevant polymer-based hydrophilic nanoparticles. Most in vivo drug delivery and imaging applications have proposed the use of nanoparticles with hydrophilic "stealth" surfaces [often achieved through poly(ethylene glycol) (PEG)-based surface modifications] as well as neutral to anionic surface charge, primarily to allow longer in vivo circulation time by reducing protein adsorption and rapid clearance by the reticuloendothelial system (2, 24–27). These nanocarriers are useful for delivering a wide variety of hydrophilic and hydrophobic drugs (small molecules, proteins, or nucleic acids) to target sites, e.g., tumors with potential to significantly reduce side effects (28). However, it is unclear how cellular internalization of hydrophilic, anionic particles varies with particle geometry and how their kinetics and uptake mechanisms differ with particle shape at the nanoscale. Further, it is unclear whether shape effects are consistent throughout different mammalian cell types. Once nanoparticles are injected into blood vessels, they encounter and interact with various cells types including endothelial cells, immune cells, and epithelial cells, all performing different physiological functions. It is hence paramount to characterize the effect of particle shape on these various cell types.

Here we present a comprehensive in vitro study showing the complex interplay between shape and size of anionic nanohydrogels on their uptake in epithelial, endothelial, and immune cells. Specifically, we compare nanoscale discoidal and rod-shaped PEG-based hydrogel particles of equivalent volume and dimensions in various cell lines and show that compared with spherical particles, these nanodiscs and nanorods have unique, geometry-dependent, cell type-specific internalization kinetics and uptake mechanisms.

Results and Discussion

Fabrication of Hydrophilic, Anionic Nanoparticles of Equivalent Volume and Charge. Understanding the effect of nanoscale geometry on cell uptake requires highly monodispersed, shape- and size-specific

Significance

Nanoparticles are widely investigated for intracellular drug delivery and molecular imaging and should be designed to maximize cell uptake. Here the effects of particle geometry to maximize nanoparticle uptake by mammalian cells are evaluated. The findings show that uptake is governed by a combination of cell–particle adhesion, strain energy for membrane wrapping around the particle, and local particle concentration at the cell membrane, all of which are particle-shape–dependent. Under typical culture conditions, disc-shaped hydrophilic nanoparticles were internalized more efficiently than nanorods. Interestingly, larger nanodiscs and rods had higher uptake compared with the smallest particles tested. Mechanisms of uptake were also shape- and cell type-specific. These results provide important insights for rational design of nanocarriers to maximize intracellular delivery efficacy.

Author contributions: R.A., V.S., P.J., L.S., S.V.S., and K.R. designed research; R.A., V.S., and P.J. performed research; P.J. and L.S. contributed new reagents/analytic tools; R.A., V.S., and P.J. analyzed data; and R.A., V.S., P.J., L.S., S.V.S., and K.R. wrote the paper.

Conflict of interest statement: S.V.S. is a founder and Chief Scientific Officer of Molecular Imprints, Inc. (MII), Austin, TX. MII has provided nanofabrication support as part of the joint National Science Foundation Grant CMMI0900715. The authors declare no financial conflict of interest.

This article is a PNAS Direct Submission. W.M.S. is a guest editor invited by the Editorial Board.

[1]Present address: The Wallace H. Coulter Department of Biomedical Engineering, Georgia Institute of Technology, Atlanta, GA 30332.

[2]To whom correspondence should be addressed. E-mail: krish.roy@gatech.edu.

This article contains supporting information online at www.pnas.org/lookup/suppl/doi:10.1073/pnas.1305000110/-/DCSupplemental.

nanoparticles of equivalent volumes and identical surface properties and material compositions. These particles should also have minimal interference from serum protein adsorption and electrostatic adsorption with cell membranes.

We have previously reported the use of Jet and Flash Imprint Lithography (J-FIL) for top down fabrication of monodisperse, biocompatible, polyethylene glycol diacrylate (PEGDA)-based hydrogel nanoparticles of precise sizes and shapes (8, 29, 30). These shape-specific particles were shown to encapsulate a variety of biomolecules including antibodies, nucleic acids, and anticancer drugs (Doxorubicin) and exhibit enzyme-triggered drug release.

Using this process, we fabricated PEGDA-based discoidal [220-nm diameter (d) × 100-nm height (h), 325-nm d × 100-nm h, and 80-nm d × 70-nm h] and cuboidal (rod-shaped) nanoparticles (100 × 100 × 400 nm and 100 × 100 × 800 nm) (Fig. 1 *A*–*G*). The 220 × 100-nm discs and 100 ×100 × 400-nm rods as well as the 325 × 100-nm discs and 100 ×100 × 800-nm rods represent particles of similar volumes and similar largest surface area, although the difference between their largest dimensions is significant. All particles had an average zeta potential of about −57 mV (Fig. 1*H*) which along with the material composition (PEGDA) ensured minimal aggregation in serum (*SI Appendix*, Fig. S1 and Table S1) as well as minimized electrostatic adsorption to negatively charged cell membranes.

Nanoparticle Internalization: Epithelial Cells Prefer Nanodiscs over Nanorods Under Typical Upright in Vitro Conditions. For uptake studies, a low concentration of nanoparticles (5 μg/mL) was used. Particles were tested with various cell lines for cytotoxicity and found to be nontoxic (*SI Appendix*, Fig. S2). All nanoparticles were synthesized with fluorescein-acrylate, such that fluorescein molecules are covalently attached to and distributed throughout the nanoparticle matrix. Particles were administered to cells in culture at equal total fluorescence intensity (to mimic equal drug dosage) which also corresponded to an equal particle mass [verified using thermogravimetric analyzer (TGA), *SI Appendix*, Fig. S3].

Uptake studies were performed on HeLa cells, and particle internalization was qualitatively assessed using confocal microscopy (*SI Appendix*, Fig. S4). For quantitative analysis, flow cytometry was performed, and data showing median fluorescence increase (over untreated cells) in cells were captured over time (Fig. 2*A*). Between discoidal and rod-shaped nanoparticles of similar volume, nanodiscs were more efficiently internalized at all time points. Interestingly, Barua et al. (22) reported that for nonspecific hydrophobic polystyrene particles, nanorods and nanodiscs have similar uptake in epithelial breast cancer cells. These differences could highlight the effect of hydrophobic versus hydrophilic surfaces as well as cell types evaluated and emphasize the importance of material composition in understanding nanoparticle-mediated intracellular delivery. In addition, the nanorods used in our study have a cuboidal cross section, whereas those used by Barua et al. (22) are nanoellipsoids. Furthermore, in our studies, for both discs and rods, nanoparticles with larger volumes were taken up more effectively compared with their smaller counterparts. This is counterintuitive compared with spherical polymer particles where smaller particles show higher uptake in HeLa cells (5, 6) (*SI Appendix*, Fig. S5*A*). Although Huang et al. (18) have shown similar effect with rod-shaped mesoporous silica particles in human melanoma A375 cells, this has not been previously reported for polymeric nanodiscs or nanorods. To ensure that this is not cell line-specific, these experiments were repeated on another epithelial cell line, HEK 293, and similar trends were observed (Fig. 2*B* and *SI Appendix*, Fig. S5*B*).

Uptake Kinetics and Efficiency of Nanoparticles Is Cell Type-Specific. To determine the effect of particle shape on other types of cells that nanoparticles may encounter in vivo, human umbilical vein endothelial cells (HUVECs) and primary mouse bone marrow dendritic cells (BMDCs) were used. BMDCs showed similar disc versus rod uptake preference to that of epithelial cells (Fig. 2*C*); that is, nanodiscs were internalized more efficiently than nanorods, and larger particles were internalized more than smaller ones. HUVEC cells, however, showed unique trends wherein intermediately sized discs (220-nm d) were internalized more efficiently than either smaller- or larger-volume discs as well as nanorods (Fig. 2*D*). Surprisingly, although the nanoparticle-to-cell ratio was 10 times less than that used in epithelial cells, the median fluorescence values were similar, indicating significantly higher uptake efficacy in endothelial cells. This 10 times lower dose was used to keep similar median fluorescence values of uptake across the different cell lines. This allows effective comparison of uptake kinetics between different cells and avoids saturation. Decrease in median fluorescence observed at 48 h in HUVECs could be a result of faster particle dilution per cell because of cell division and low particle dose or due to endothelial cell-specific exocytosis (31). Although these PEGDA particles are not degradable in water in the time frame studied, oxidative degradation inside some cells could also be a possible cause of the observed fluorescence decrease. Mice lung microvasculature endothelial cells were also shown to follow a similar trend where 220-nm-d discs were more efficiently internalized compared with 400-nm rods (*SI Appendix*, Fig S6).

All uptake experiments were repeated several times using nanohydrogels manufactured in different batches and cells of different passage numbers (passage 3 to18; representative reproducible results are shown in *SI Appendix*, Fig. S7).

Further, assuming that fluorescein-acrylate is uniformly distributed throughout the particle matrix, we estimated the relative number of particles present per cell (normalized to 80-nm-d discs) at the maximum internalization time points. The 220- and 325-nm-d discs have similar volumes to the 400- and 800-nm rods, respectively. Thus, for these particles, equal fluorescence administration also means administration at equal numbers. We found that between 220-nm discs and 400-nm rods, nanodiscs were internalized more efficiently than nanorods in all cell types (Fig. 2*E*). Similarly, as shown in Fig. 2*F*, for the larger, equivalent volume disc-rod pair (325-nm discs, 800-nm rods), 40–60% more disc-shaped particles were internalized in epithelial and immune cells. Interestingly, this trend is reversed in endothelial cells,

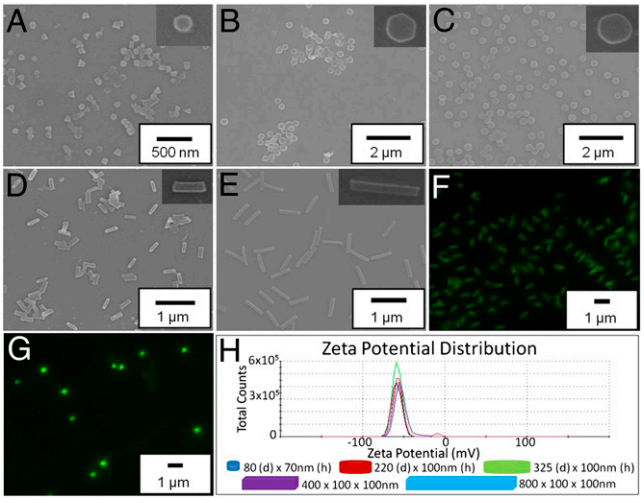

Fig. 1. Nanoparticle characterization—specific shapes, uniform fluorescence, and equivalent surface charge: SEM micrograph of (*A*) 80-nm-d × 70-nm-h discs, (*B*) 220-nm-d × 100-nm-h discs, (*C*) 325-nm-d × 100-nm-h discs, (*D*) 400 × 100 × 100-nm rods, and (*E*) 800 × 100 × 100-nm rods done by drying the samples on a silicon substrate. Fluorescence images of (*F*) 800 × 100 × 100-nm rods and (*G*) 325-nm-d × 100-nm-h discs. (*H*) Zeta potential plot for all particles (courtesy Claudia Mujat, Malvern, Inc., Westborough, MA).

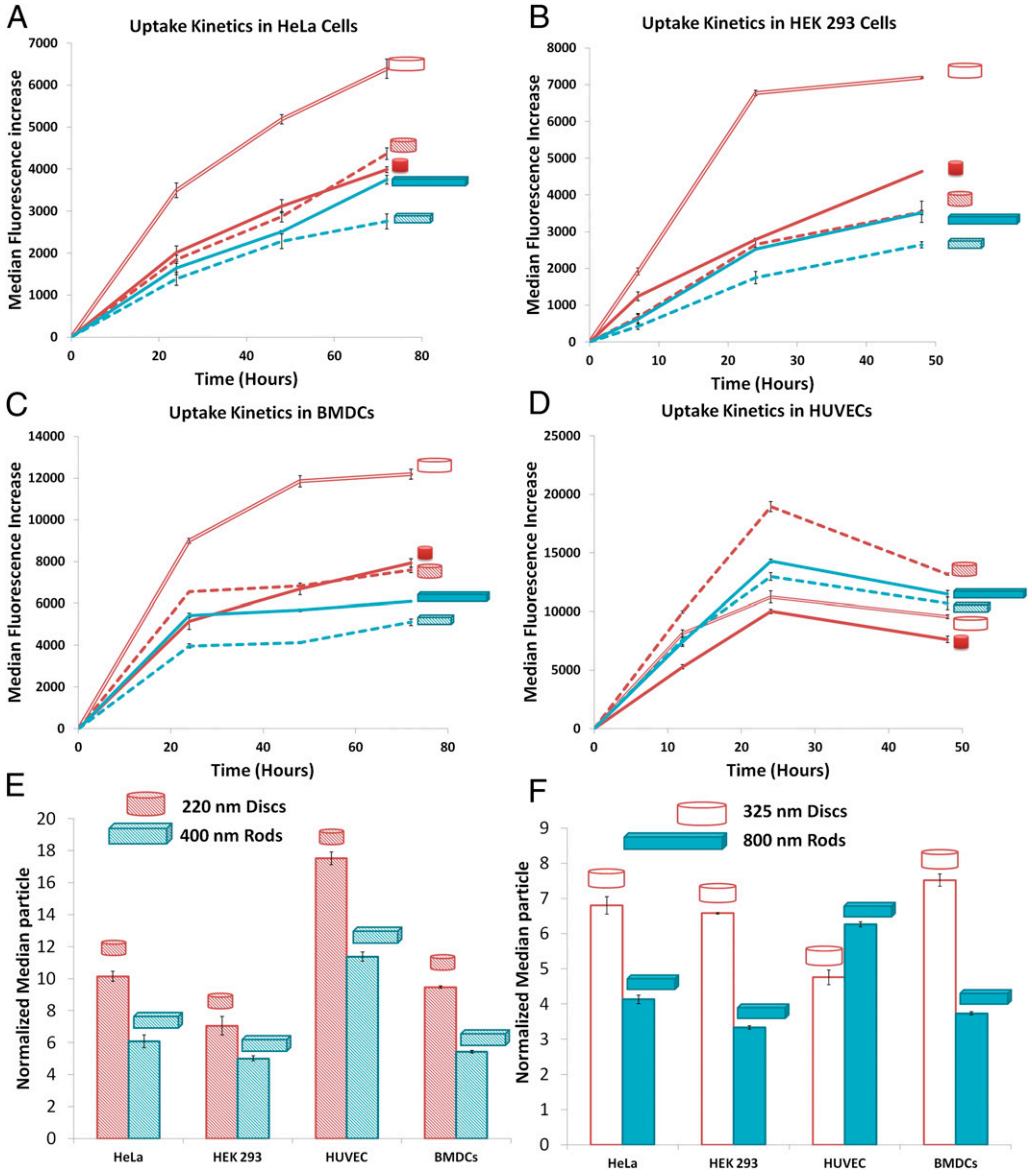

Fig. 2. Cellular-uptake kinetics of different shape-specific nanoparticles in various cell lines. (*A*) HeLa cells, (*B*) HEK 293 cells, (*C*) BMDCs, and (*D*) HUVEC cells. In *A–D*, red lines are for nanodiscs (hollow for 325 × 100-nm discs, dashed for 220 × 100-nm discs, and solid for 80 × 70-nm discs), and blue lines are for nanorods (dashed for 400 × 100 × 100-nm rods and solid for 800 × 100 × 100-nm rods). Error bars are SD with $n = 3$ for each data point. (*E–F*) Normalized median particle uptake per cell (indicates relative number of particles internalized by cells when normalized to 100 particles of 80 × 70-nm discs) at the maximum internalization time point (72 h for HeLa and BMDC, 48 h for HEKs, and 24 h for endothelial cells).

although less significantly, further confirming that the effect of particle geometry is cell type-specific.

Cell Uptake of Nanoparticles Is an Interplay Between Sedimentation, Surface Contact Area, and Strain Energy for Membrane Deformation. It has been previously reported that sedimentation plays an important role when performing in vitro cell-uptake studies with nanoparticles (32, 33). However, most studies on particle shape have not looked at the effect of gravity on in vitro cell uptake. Nanoparticles can form concentration gradients under the influence of gravity and result in higher concentrations of larger particles near the bottom surface of well plates (32). This could be a significant factor as to why larger discs and rods, with more weight per particle, are internalized more efficiently compared with smaller discs and rods.

To study whether sedimentation alone can explain the observed shape dependency of our nanohydrogels, uptake studies were performed in an inverted culture model (Fig. 3*A*). It is important to note that in inverted cell cultures, the effect of sedimentation is reversed; that is, larger particles are at a lower concentration near the cell surface compared with smaller particles which should reverse the trend seen in our noninverted uptake experiments. However, as shown in Fig. 3 *C–D* and *SI Appendix*, Fig. S8, although overall uptake efficiency decreased significantly for all shapes and sizes in inverted cultures, smaller nanodiscs or rods did not exhibit significantly higher uptake compared with their larger counterparts. In most cases, larger particles still exhibited higher uptake. Furthermore, when spherical polystyrene (PS) beads were used as control particles, smaller-diameter nanospheres, despite their lower sedimentation, showed higher uptake compared with larger-diameter beads (Fig. 3*B* and, as reported previously; ref. 32), a trend similar to that in noninverted cultures. Therefore, sedimentation effects alone cannot explain the observed internalization kinetics of disc- and

rod-shaped hydrogel nanoparticles, indicating that the effect of shape is manifested through multiple forces that together can play an important role.

One possible explanation is that for disc- and rod-shaped nanoparticles, larger size provides larger surface-contact areas for multivalent interactions with cell membranes (22, 34). This effect may allow larger adhesion forces with particles and increase the probability of initiating cellular uptake. For spherical nanoparticles, such interactions are minimal as there is a smaller contact area irrespective of the size of the nanoparticle. However, this effect of higher surface contact area alone may not be adequate to explain the difference in uptake observed between equal-volume disc and rod pairs used here because they only differ by 5% in the surface area of their largest face. Another critical parameter that could explain the difference seen between equal-volume nanodiscs and nanorods is the strain energy needed for membrane bending around nanoparticles. As shown in *SI Appendix*, *SI Text*, discs require less energy compared with rods of equal volume, and larger-diameter spheres are less favorable compared with smaller-diameter spheres.

Based on these observations, we hypothesize that in an in vitro culture system, three parameters play an important role for intracellular uptake of particles: contact or adhesion force between the nanoparticle surface and the cell membrane (governed by the shape of particles), sedimentation (governed by the weight of particles), and strain energy required for membrane deformation (governed by the shape of particles). In the upright configuration, gravity results in a higher concentration of larger particles. Larger particles also have a larger contact area to trigger membrane response. These two factors favor the uptake of larger particles. However, smaller spheres are still taken up more than the larger spheres in the upright configuration, because the strain energy cost is higher for larger spheres, and this effect dominates over the effects of concentration and contact area. In comparison, the contact area increases more with increasing sizes for the case of rods and discs than for spheres, so that the effect of contact area can become dominant and result in increased uptake of rods and discs with increasing size. For rods and discs with the same volume and surface area, the strain energy cost for uptake is higher for rods, so that discs are taken up more than rods. A similar explanation can be deduced for HUVECs; however, the contact force and strain energy would be different for different membrane compositions, and hence different trends were observed. Here intermediate-diameter discs were found to be most taken up, which, however, compared with 325-nm discs, has less sedimentation and contact surface area and more favorable strain energy values.

In the inverted configuration, the local particle concentration can be higher for smaller particles than for larger particles. In addition, the strain energy cost is smaller for smaller particles. These two effects are more important than the contact area for spheres, so that smaller spheres are still taken up more. However, for the case of rods and discs, the contact area increases more with increasing particle size than is the case for the spheres so that this effect is the dominant one and results in the observations that *i*) the smallest discs and rods are taken up the least and *ii*) the difference in uptake between discs and rods of the same volume/area is small.

Future studies need to be conducted to evaluate whether the observed shape-specific differences in uptake seen in our in vitro studies have in vivo relevance. Recently, Kolhar et al. (23) used shape-specific antibody-conjugated polystyrene particles to show that between antibody-conjugated rods and spheres, rods adhered to targeted microchannels about 2x better than spheres in vitro. These results also correlated well in vivo where rods were able to significantly enhance brain and lung endothelium targeting compared with spheres. Whether this increased targeting in vivo would lead to enhanced therapeutic effects remains to be seen; however, the study does confirm that in vitro enhancement in efficacy could correlate to corresponding in vivo results.

In Epithelial Cells, Nanodiscs Use Unique Uptake Pathways Compared with Nanorods. To further understand the specific mechanisms involved in cellular internalization of anionic nanohydrogels, pharmacological inhibitors were used to interfere with various uptake pathways. It should be noted that inhibitory effects of these agents are cell-type-dependent (35). Five types of inhibitors were chosen based on their selectivity and applications (Fig. 4*A*). Specifically, chlorampramazine, a cationic drug which results in loss of clathrin and AP2 adaptor complex protein from the cell surface and blocks specifically the clathrin-mediated pathway (36). Filipin causes aggregation of cholesterol in biological membranes and causes disruption of caveolar pits while still allowing other mechanisms (36). Amiloride blocks Na^+/H^+ exchange in cell

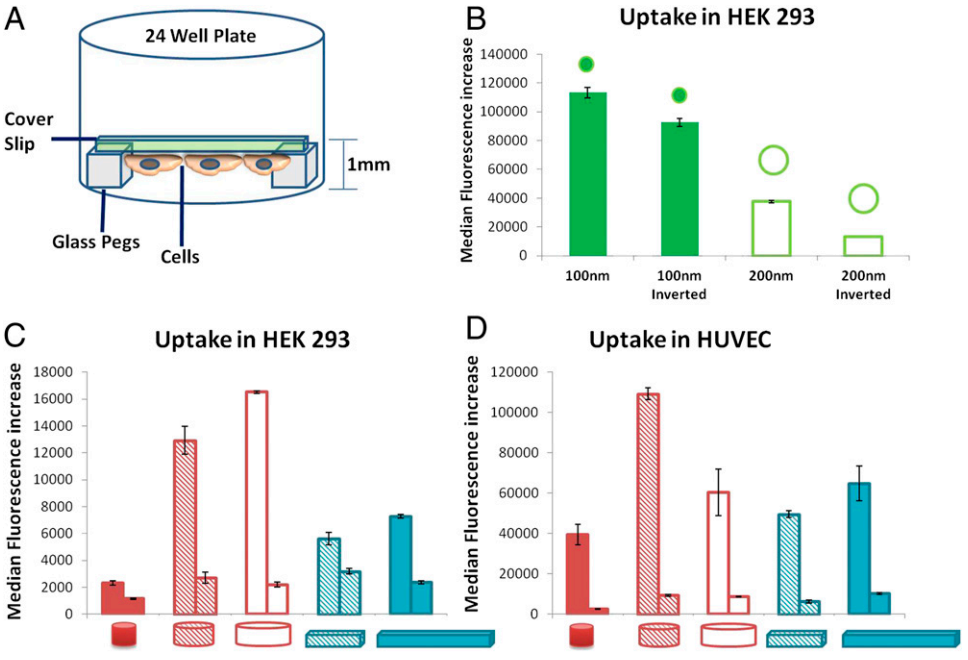

Fig. 3. Inverted culture uptake studies: Shape still matters. (*A*) Experimental setup for uptake studies in inverted conditions. (*B*) Inverted cellular uptake of spherical polystyrene beads after 24 h in HEK 293. Inverted cellular uptake of shape-specific nanoparticles after 24 h in (*C*) HEK 293 cells and (*D*) HUVEC cells. In *B*, hollow green bars are for 200-nm-*d* spherical polystyrene beads, and solid green bars are for 100-nm-*d* spherical polystyrene beads. In *C* and *D*, for each set of bars, the left bar represents upright, and the right bar represents inverted configuration. Red bars are for discs (hollow red bars for 325 × 100-nm discs, dashed red bars for 220 × 100-nm discs, and solid red bars for 80 × 70-nm discs), and blue bars are for rods (dashed blue bars for 400 × 100 × 100 nm and solid blue bars for 800 × 100 × 100 nm). Error bars are SD with $n = 3$ for each data point.

membranes, whereas cytochalasin D blocks actin polymerization and hence blocks membrane ruffling and macropinocytosis. However, actin filaments are involved in various other endocytic pathways; hence, inhibition by cytochalasin D is not very specific (36). Nocodazole hinders microtubule polymerization and, hence, vesicular transport (37).

Inhibitor concentrations were optimized to achieve a minimum of 90% cell viability over 8 h for HEK and HeLa (epithelial cells) and HUVEC (endothelial cells). For all inhibitor studies, particles were administered for 6 h. Prolonged exposure to pharmacological inhibitors causes cell death, as these reagents are toxic to cells. To allow sufficient uptake at the 6-h time point, particles were administered at five times higher dose. This allowed sufficient uptake of particles to use pharmacological inhibitors without causing significant toxicity (*SI Appendix*, Fig. S9). In all cell types (Fig. 3 *B–C* and *SI Appendix*, Fig. S10), macropinocytosis was found to be the common internalization pathway. Interestingly, in HEK cells, nanodiscs (but not nanorods) were also internalized using caveolae-mediated endocytosis. This could partially explain why discs outperform rods in these cells. However, such a shape-specific internalization mechanism was not seen in HeLa cells (*SI Appendix*, Fig. S10) where both discs and rods were internalized by a caveolae-mediated pathway, further demonstrating that similar types of cells from different organs (i.e., epithelial cells from kidney vs. cervix) behave differently. It has been previously reported that negatively charged particles are internalized by a caveolae-mediated pathway in epithelial cells (27, 38–40). Additionally, as the caveolae pathway is involved in transcytosis, this has further significant implications in delivering therapeutic and diagnostic agents across epithelial barriers (41).

Clathrin-Mediated Uptake Is Used by Endothelial Cells but Not by Epithelial Cells. In contrast to epithelial cells, HUVECs used both macropinocytosis and clathrin-mediated pathways for both nanorods as well as nanodiscs and were affected by pathway inhibition to a larger extent than epithelial cells. This can either indicate a more efficient role these two pathways play in nanoparticle uptake or a more complete inhibition in HUVECs. To further confirm that the clathrin pathway was indeed not involved in epithelial cells, confocal microscopy images were gathered with an epithelial cell line (retinal pigment epithelium (RPE) cells) where the clathrin is labeled with a red fluorescent tag (mCherry). Confocal imaging showed little to no colocalization of the green-labeled nanoparticles with clathrin pits (*SI Appendix*, Fig. S11), supporting the results from pharmacological inhibitor studies. For spherical PS beads of different sizes (100, 200, and 500 nm; *SI Appendix*, Fig. S12), the inhibition studies indicated that cells use multiple uptake pathways for nanospheres depending on their size, including clathrin-mediated (200 and 500 nm), macropinocytosis (all sizes), and caveolae-mediated (200 nm). It should be noted that the PS beads used have different surface and bulk material composition compared with the nonspherical nanoparticles.

In conclusion, we demonstrate that nanoparticle shape along with size plays a critical role in cellular uptake of hydrophilic

A

Inhibitor	Cellular Mechanism Inhibited	Concentration used		Time used
		HEK 293	HUVEC	
Chlorpromazine	Clathrin	30μM	28μM	6 hour
Amiloride	Macropinocytosis	850μM	800μM	6 hour
Cystochalsin D	Macropinocytosis	150nM	500nM	6 hour
Nocodazole	Microtubules	20μM	13μM	6 hour
Filipin	Caveolae	50μg/ml	40μg/ml	6 hour

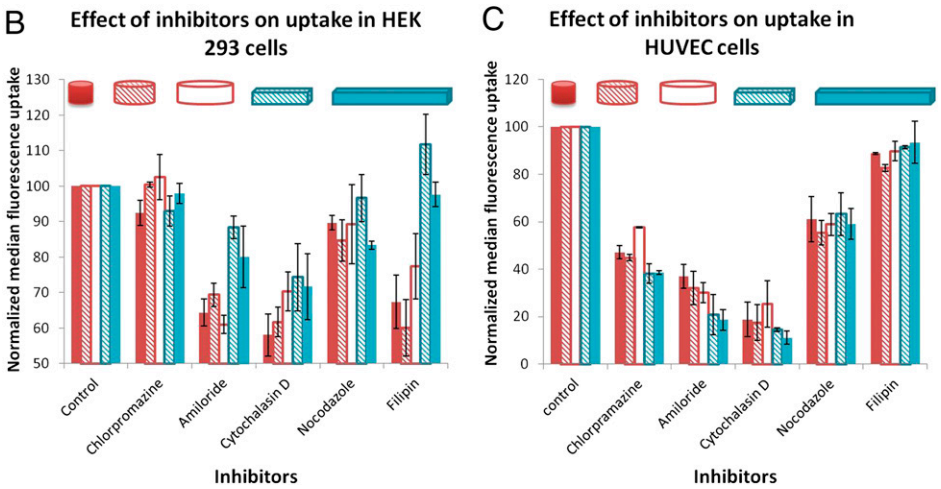

Fig. 4. Effect of pharmacological inhibitors on uptake of various shape-specific nanoparticles. (*A*) Inhibitors used (with function, concentration, and time) for the uptake experiments. (*B–C*) Change in normalized median fluorescence uptake of shape-specific particles due to presence of inhibitors in HEK 293 and HUVEC cells. Error bars are SD with $n = 5$ for each data point. Red bars are for nanodiscs (solid for 80-nm-*d* discs, dashed for 220-nm-*d* discs, and hollow for 325-nm-*d* discs), and blue lines are for nanorods (dashed for 400 × 100 × 100-nm rods and solid for 800 × 100 × 100-nm rods).

polymer nanocarriers. The effect of shape and size is manifested through the interplay of three parameters: *i*) contact area or adhesion forces between the particle surface and cell membranes, *ii*) the strain energy required for membrane deformation around the particle, and *iii*) effect of sedimentation or local particle concentration at the cell surface. In all cell types tested, nanodiscs of larger or intermediate sizes were internalized more efficiently compared with nanorods or the smallest-size discs. Furthermore, we show that cellular mechanisms for nanohydrogel uptake vary significantly with particle geometry and are cell type-specific. We propose that when nanoparticle surface properties and composition are kept constant, each cell type can "sense" the nanoscale geometry (both shape and size) and trigger unique uptake pathways and thus have different shape-dependent internalization efficiencies. These results provide fundamental insights on the effect of nanoscale shape on cell uptake and offer unique opportunities for the use of particle geometry as a design criterion to control cellular internalization and affect cell targeting, therapeutics, and diagnostics delivery, as well as nanotoxicity.

Methods

Nanoparticles were fabricated using jet and flash imprint lithography (JFIL) on silicon wafers. Nanoimprinted and etched particles were released from wafer in water and dialyzed. Uptake was quantified using flow cytometry both in upright and inverted cultures. For detailed methods, please refer to *SI Appendix*.

ACKNOWLEDGMENTS. We thank Dr. Daniel Sellan and Dr. Jeanne Stachowiak of The University of Texas (UT) at Austin for helpful discussions on strain energy calculations and Ms. Jardin Leleux for bone marrow dendritic cell isolation and culture. Zeta potential analysis was performed by Dr. Claudia Mujat (Malvern, Inc.), mCherry-labeled clathrin retinal pigment epithelium cells were a gift from Dr. Marcel Mettlen and Dr. Sandra Schmid (UT Southwestern Medical Center), and mouse lung endothelial cells were a gift from Dr. Aaron Baker's laboratory (UT Austin). Nanofabrication and metrology were conducted at Molecular Imprints, Inc. and the Microelectronics Research Center (MRC). We also acknowledge support from the Texas Materials Institute, the Center for Nano and Molecular Science, and the Institute for Cellular and Molecular Biology (UT Austin). This work was supported in part through National Science Foundation Grant CMMI0900715 (nanomanufacturing) and National Institutes of Health Grant EB008835 (initial feasibility study). The MRC (UT Austin) is a member of the National Nanotechnology Infrastructure Network.

1. Janib SM, Moses AS, MacKay JA (2010) Imaging and drug delivery using theranostic nanoparticles. *Adv Drug Deliv Rev* 62(11):1052–1063.
2. Petros RA, DeSimone JM (2010) Strategies in the design of nanoparticles for therapeutic applications. *Nat Rev Drug Discov* 9(8):615–627.
3. Tseng P, Judy JW, Di Carlo D (2012) Magnetic nanoparticle-mediated massively parallel mechanical modulation of single-cell behavior. *Nat Methods* 9(11):1113–1119.
4. Nel A, Xia T, Mädler L, Li N (2006) Toxic potential of materials at the nanolevel. *Science* 311(5761):622–627.
5. He C, Hu Y, Yin L, Tang C, Yin C (2010) Effects of particle size and surface charge on cellular uptake and biodistribution of polymeric nanoparticles. *Biomaterials* 31(13): 3657–3666.
6. Chithrani BD, Ghazani AA, Chan WC (2006) Determining the size and shape dependence of gold nanoparticle uptake into mammalian cells. *Nano Lett* 6(4):662–668.
7. Rodriguez PL, et al. (2013) Minimal "Self" peptides that inhibit phagocytic clearance and enhance delivery of nanoparticles. *Science* 339(6122):971–975.
8. Agarwal R, et al. (2012) Scalable imprinting of shape-specific polymeric nanocarriers using a release layer of switchable water solubility. *ACS Nano* 6(3):2524–2531.
9. Rolland JP, et al. (2005) Direct fabrication and harvesting of monodisperse, shape-specific nanobiomaterials. *J Am Chem Soc* 127(28):10096–10100.
10. Buyukserin F, Aryal M, Gao J, Hu W (2009) Fabrication of polymeric nanorods using bilayer nanoimprint lithography. *Small* 5(14):1632–1636.
11. Champion JA, Mitragotri S (2006) Role of target geometry in phagocytosis. *Proc Natl Acad Sci USA* 103(13):4930–4934.
12. Tasciotti E, et al. (2008) Mesoporous silicon particles as a multistage delivery system for imaging and therapeutic applications. *Nat Nanotechnol* 3(3):151–157.
13. Geng Y, et al. (2007) Shape effects of filaments versus spherical particles in flow and drug delivery. *Nat Nanotechnol* 2(4):249–255.
14. Gratton SE, et al. (2008) The effect of particle design on cellular internalization pathways. *Proc Natl Acad Sci USA* 105(33):11613–11618.
15. Jiang X, et al. (2013) Plasmid-templated shape control of condensed DNA-block copolymer nanoparticles. *Adv Mater* 25(2):227–232.
16. Decuzzi P, Pasqualini R, Arap W, Ferrari M (2009) Intravascular delivery of particulate systems: Does geometry really matter? *Pharm Res* 26(1):235–243.
17. Chauhan VP, et al. (2011) Fluorescent nanorods and nanospheres for real-time in vivo probing of nanoparticle shape-dependent tumor penetration. *Angew Chem Int Ed Engl* 50(48):11417–11420.
18. Huang X, Teng X, Chen D, Tang F, He J (2010) The effect of the shape of mesoporous silica nanoparticles on cellular uptake and cell function. *Biomaterials* 31(3):438–448.
19. Shah S, Liu Y, Hu W, Gao J (2011) Modeling particle shape-dependent dynamics in nanomedicine. *J Nanosci Nanotechnol* 11(2):919–928.
20. Smith BR, et al. (2012) Shape matters: intravital microscopy reveals surprising geometrical dependence for nanoparticles in tumor models of extravasation. *Nano Lett* 12(7):3369–3377.
21. Rothemund PW (2006) Folding DNA to create nanoscale shapes and patterns. *Nature* 440(7082):297–302.
22. Barua S, et al. (2013) Particle shape enhances specificity of antibody-displaying nanoparticles. *Proc Natl Acad Sci USA* 110(9):3270–3275.
23. Kolhar P, et al. (2013) Using shape effects to target antibody-coated nanoparticles to lung and brain endothelium. *Proc Natl Acad Sci USA* 110(26):10753–10758.
24. Brannon-Peppas L, Blanchette JO (2004) Nanoparticle and targeted systems for cancer therapy. *Adv Drug Deliv Rev* 56(11):1649–1659.
25. Albanese A, Tang PS, Chan WC (2012) The effect of nanoparticle size, shape, and surface chemistry on biological systems. *Annu Rev Biomed Eng* 14:1–16.
26. Peer D, et al. (2007) Nanocarriers as an emerging platform for cancer therapy. *Nat Nanotechnol* 2(12):751–760.
27. Agarwal R, Roy K (2013) Intracellular delivery of polymeric nanocarriers: A matter of size, shape, charge, elasticity and surface composition. *Ther Deliv* 4(6):705–723.
28. Hamidi M, Azadi A, Rafiei P (2008) Hydrogel nanoparticles in drug delivery. *Adv Drug Deliv Rev* 60(15):1638–1649.
29. Caldorera-Moore M, et al. (2011) Swelling behavior of nanoscale, shape- and size-specific, hydrogel particles fabricated using imprint lithography. *Soft Matter* 7(6): 2879–2887.
30. Glangchai LC, Caldorera-Moore M, Shi L, Roy K (2008) Nanoimprint lithography based fabrication of shape-specific, enzymatically-triggered smart nanoparticles. *J Control Release* 125(3):263–272.
31. Bartczak D, Nitti S, Millar TM, Kanaras AG (2012) Exocytosis of peptide functionalized gold nanoparticles in endothelial cells. *Nanoscale* 4(15):4470–4472.
32. Cho EC, Zhang Q, Xia Y (2011) The effect of sedimentation and diffusion on cellular uptake of gold nanoparticles. *Nat Nanotechnol* 6(6):385–391.
33. Teeguarden JG, Hinderliter PM, Orr G, Thrall BD, Pounds JG (2007) Particokinetics in vitro: Dosimetry considerations for in vitro nanoparticle toxicity assessments. *Toxicol Sci* 95(2):300–312.
34. Muro S, et al. (2008) Control of endothelial targeting and intracellular delivery of therapeutic enzymes by modulating the size and shape of ICAM-1-targeted carriers. *Mol Ther* 16(8):1450–1458.
35. Vercauteren D, et al. (2010) The use of inhibitors to study endocytic pathways of gene carriers: optimization and pitfalls. *Mol Ther* 18(3):561–569.
36. Ivanov AI (2008) Pharmacological inhibition of endocytic pathways: Is it specific enough to be useful? *Methods Mol Biol* 440:15–33.
37. dos Santos T, Varela J, Lynch I, Salvati A, Dawson KA (2011) Effects of transport inhibitors on the cellular uptake of carboxylated polystyrene nanoparticles in different cell lines. *PLoS ONE* 6(9):e24438.
38. Harush-Frenkel O, Rozentur E, Benita S, Altschuler Y (2008) Surface charge of nanoparticles determines their endocytic and transcytotic pathway in polarized MDCK cells. *Biomacromolecules* 9(2):435–443.
39. Sahay G, Kim JO, Kabanov AV, Bronich TK (2010) The exploitation of differential endocytic pathways in normal and tumor cells in the selective targeting of nanoparticulate chemotherapeutic agents. *Biomaterials* 31(5):923–933.
40. Sahay G, Alakhova DY, Kabanov AV (2010) Endocytosis of nanomedicines. *J Control Release* 145(3):182–195.
41. Kim KJ, Malik AB (2003) Protein transport across the lung epithelial barrier. *Am J Physiol Lung Cell Mol Physiol* 284(2):L247–L259.